A POSTERIORI ERROR ESTIMATION FOR A NODAL METHOD IN NEUTRON TRANSPORT CALCULATIONS

Gustavo C. Buscaglia*, Oscar M. Zamonsky*, and Yousry Y. Azmy†

*Centro Atómico Bariloche and Instituto Balseiro
8400-Bariloche, RN, Argentina
gustavo@cab.cnea.gov.ar, zamonsky@cab.cnea.gov.ar

†Oak Ridge National Laboratory
Oak Ridge, Tennessee 37831-6363, USA
yya@ornl.gov

Key words: Nodal methods, Neutron transport, a posteriori error estimation.

Abstract. *An a posteriori error analysis of the spatial approximation is developed for the one-dimensional Arbitrarily High Order Transport-Nodal method. The error estimator preserves the order of convergence of the method when the mesh size tends to zero with respect to the L^2 norm. It is based on the difference between two discrete solutions that are available from the analysis. The proposed estimator is decomposed into error indicators to allow the quantification of local errors. Some test problems with isotropic scattering are solved to compare the behavior of the true error to that of the estimated error.*

1 INTRODUCTION

This paper briefly overviews some recent advances in what regards nodal methods for the neutron transport equation. Numerical methods in neutronics are very specific, and in general not familiar to the Computational Mechanics community. Care was taken to avoid technicalities, adapt the notation and remark features that could prove useful in other areas.

High order nodal methods produce highly accurate solutions with high computational efficiency in one and multidimensional geometry problems. In particular, the simple form of the equations of the Arbitrarily High Order Transport-Nodal Method (AHOT-N) proposed by Azmy[1] makes these methods very attractive for practical purposes. The multidimensional AHOT-N method is developed by transversely averaging the transport equation and solving the 1D resulting equations. This motivated us to analyze the 1D AHOT-N method.

The neutron transport equation, in 1D, can be written as

$$\underline{\underline{\mu}}\frac{d\underline{\psi}}{dx}(x)+\sigma(x)\underline{\psi}(x)=\sigma(x)\underline{\underline{S}}(x)\underline{\psi}(x)+\underline{q}(x), \tag{1}$$

where $\underline{\psi}$ is the vector of angular fluxes (an S_n approximation is assumed), $\underline{\underline{\mu}}$ the (diagonal) matrix of direction cosines, σ the total cross-section, $\underline{\underline{S}}$ the scattering matrix and $\underline{q}$ the external source. Boundary conditions are given for each component ψ_i at the left (x=0) or right (x=L) boundaries, depending on the sign of μ_i (if positive at the left, if negative at the right). If we denote by L the differential operator (comprising boundary conditions) on the left-hand side of (1) and by S the scattering operator on the right, we arrive, formally, at

$$\mathsf{L}\underline{\psi}=\mathsf{S}\underline{\psi}+\underline{q} \tag{2}$$

To introduce the method we need to define a finite dimensional subspace $\tilde{V}$ of $C_p^N(0,L)$, the latter being the space of N-tuples of functions in $(0,L)$ with continuous derivatives up to order p. Let the domain $[0,L]$ be partitioned into a finite number of non-overlapping cells $\{C_k, k=1,...,K\}$ and let $\tilde{V}$ be defined as the subspace of $C_p^N[0,L]$ such that each component is

a polynomial of degree $\leq \Lambda$ in each C_k. No continuity is imposed at the cell interfaces for elements of $\tilde{V}$. The dimension of $\tilde{V}$ is clearly $NK(\Lambda+1)$.

Let Π be the L^2-orthogonal projection from $C_p^N[0,L]$ onto $\tilde{V}$, namely

$$\int_0^L \left(\underline{g}(x) - \Pi\underline{g}(x)\right)\cdot\underline{\tilde{v}}(x)dx = 0 \qquad \forall\underline{\tilde{v}}\in\tilde{V}. \tag{3}$$

For simplicity, $\Pi\underline{g}$ will alternatively be denoted by $\underline{\tilde{g}}$. We are now in a position to introduce the AHOT-N method. Let $\underline{\hat{\psi}} = (\hat{\psi}_i)$ denote the approximate solution provided by the method; it is defined by

$$\mathsf{L}\underline{\hat{\psi}} = \Pi\left[\mathsf{S}\underline{\hat{\psi}} + \underline{q}\right] = \mathsf{S}\underline{\tilde{\psi}} + \underline{\tilde{q}}. \tag{4}$$

By virtue of the remark made above, $\underline{\hat{\psi}}$ can also be viewed as the solution to

$$\underline{\underline{\mu}}\frac{d\underline{\hat{\psi}}}{dx}(x) + \sigma(x)\underline{\hat{\psi}}(x) = \sigma(x)\underline{\underline{S}}(x)\underline{\tilde{\psi}}(x) + \underline{\tilde{q}}(x) \tag{5}$$

with the boundary conditions mentioned before. Remarkably, Eq. 5 fully defines a numerical methodology which can be effectively implemented. Notice that the method keeps the differential operator unchanged, but the scattering operator and the source are projected onto a specific subspace in which the differential operator can be inverted exactly. This methodology, reminiscent of other methods in computational mechanics such as the "exact transport + projection" schemes, produces very accurate results as shown later. There exist analyses of similar approximations for some particular *fixed* low-order representations of the angular flux[2,3].

The a priori analysis of the General Order method approximation[4] proved *a priori* error estimates of order $h^{\Lambda+2}$ in the sup norm. In addition, they showed a superconvergence result at cell boundaries, order $h^{2\Lambda+2}$. Notice that an error of order $h^{\Lambda+2}$ exceeds by one the best approximation obtainable with polynomials of degree Λ. This is so because $\underline{\hat{\psi}}$ is **not** a polynomial, but instead the exact solution of Eq. 5, in which the right-hand side **is** a polynomial. The final form of the method was originally derived by Azmy[1], who developed a Weighted Diamond Difference Form for the multidimensional case making the method easier to use. From

the viewpoint of the error analysis, this method is classed within characteristic methods with exact moments[4,5]. We will not elaborate here on the implementation, referring to Azmy[1] or Zamonsky[6] for details.

2 A POSTERIORI ERROR ESTIMATION

One usually faces the problem of estimating the accuracy of the solution for a given, completed, computation. For this purpose, *a posteriori* estimates are needed. Furthermore, a natural question is how to refine the approximation to get maximal accuracy gain with minimal computing cost. The answer can be obtained via *local a posteriori* error indicators. Though the literature in *a posteriori* error estimators is vast[7,8], applications in neutronics are scarce and apply only to the diffusion equation[9,10].

Let $\underline{\varepsilon}$ be the true error, $\underline{\varepsilon} = \underline{\hat{\psi}} - \underline{\psi}$, and let $|\underline{\varepsilon}|^2 = \underline{\varepsilon} \cdot \underline{\varepsilon} = \sum_{i=1}^{N} \varepsilon_i^2$, the following bound can be proved[6]

$$\|\underline{\varepsilon}\|_{L^2}^2 \le \sum_k \frac{h_k^2}{2} \int_{x_{k-1/2}}^{x_{k+1/2}} \left(\underline{\underline{\mu}}^{-1}\left[\sigma_k \underline{\underline{S}}_k (\underline{\tilde{\psi}} - \underline{\hat{\psi}})(x') + (\underline{\tilde{q}} - \underline{q})(x')\right]\right)^2 dx' + h.o.t. \qquad (6)$$

where *h.o.t.* stands for "higher order terms". Equation (6) gives an upper bound for the error measured in L^2 norm for a general scattering operator. Since its right hand side depends only on known quantities, it can be used to estimate the global error of the solution obtained with the 1D, AHOT-N method. The estimator above has asymptotically the same order as the error, so that is does not overestimate the true error in what concerns order of convergence (the effectivity index does not tend to zero). It is known[4] that $\|\underline{\varepsilon}\|_{L^\infty} = O(h^{\Lambda+2})$. As $\|\underline{\varepsilon}\|_{L^2} \le \sqrt{L}\,\|\underline{\varepsilon}\|_{L^\infty}$, it follows that the order of $\|\underline{\varepsilon}\|_{L^2}$ is also $O(h^{\Lambda+2})$. Since $(\tilde{\psi}_i - \hat{\psi}_i) = O(h^{\Lambda+1})$ and $(\tilde{q}_i - q_i) = O(h^{\Lambda+1})$, the estimator given by the square root of the right hand side of Eq. (6) is $O(h^{\Lambda+2})$, the same as the order of the error.

Equation (6) estimates the global error, of interest is to decompose the estimator into *local error indicators*. These indicate where the approximation should be refined to improve global

accuracy at minimum expense. Let η_{ik} denote an error indicator for component i in cell C_k. By direct inspection, η_{ik} can be defined as

$$\eta_{ik}^2 \equiv \frac{h_k^2}{2} \int_{x_{k-1/2}}^{x_{k+1/2}} \left(\sigma_k \underline{\underline{\mu}}^{-1} \underline{\underline{S}}_k (\underline{\tilde{\psi}} - \underline{\hat{\psi}})(x') + \underline{\underline{\mu}}^{-1} (\underline{\tilde{q}} - \underline{q})(x') \right)_i^2 dx', \tag{7}$$

The estimator presented above is based on the difference between $\underline{\hat{\psi}}$ and $\underline{\tilde{\psi}}$, two approximations calculated in the AHOT-N method that have different accuracy, as already discussed. This reminds of "*hierarchic*" error estimators in the finite elements terminology[8]. However, the proposed estimator is a "*residual-based*" one, that is, it reduces to a suitable norm of the residual of the differential equation. To see this notice that from Eq. 5 we have

$$\sigma \underline{\underline{S}} (\underline{\tilde{\psi}} - \underline{\hat{\psi}}) + \underline{\tilde{q}} - \underline{q} = \underline{\underline{\mu}} \frac{d\underline{\hat{\psi}}}{dx} + \sigma \underline{\hat{\psi}} - \sigma \underline{\underline{S}} \underline{\hat{\psi}} - \underline{q} = \underline{R}(\underline{\hat{\psi}}). \tag{8}$$

where $\underline{R}(\underline{\psi})$ is the residual. Replacing Eq. (8) into Eq. (7) we see that the error indicator is in fact

$$\eta_{ik}^2 = \frac{h_k^2}{2} \int_{x_{k-1/2}}^{x_{k+1/2}} \left| \underline{\underline{\mu}}^{-1} \underline{R} \right|^2 dx, \tag{9}$$

where the L^2 norm of the residual has been made evident. For computational purposes, however, formula (7) is more convenient.

3 NUMERICAL EXPERIMENTS

The test problem considered here consists of an heterogeneous slab of width $L = 0.1$ meters. The left half has macroscopic total cross section $\sigma = 100\, m^{-1}$, with a scattering part of the cross section c=0.5, and unit external source. The right half has $\sigma = 200\, m^{-1}$, c=0.05, and no source. It is solved using an S_4 Gaussian quadrature. We consider several uniform partitions into K cells, with h ranging from $L/2$ to $L/128$, and expansion orders Λ from zero to ten. In Fig. 1 we compare the first exact angular flux ψ_1 to its approximations $\hat{\psi}_1$ and $\tilde{\psi}_1$ calculated with h=$L/4$ (K=4) and $\Lambda = 2$. Part (a) of the figure shows the three fluxes, while Part (b)

depicts the differences between the approximate fluxes and the exact solution. It is clear from the figure that $\hat{\underline{\psi}}$ is significantly more accurate.

A quantitative assessment of accuracy is obtained evaluating the L^2-norm of the error,

$$\varepsilon = \sqrt{\int_0^L \left|\underline{\psi}^e(x) - \underline{\psi}(x)\right|^2 dx} \quad , \qquad \tilde{\varepsilon} = \sqrt{\int_0^L \left|\underline{\psi}^e(x) - \tilde{\underline{\psi}}(x)\right|^2 dx} \, . \tag{10}$$

As no confusion can arise, we have used ε to denote the L^2-norm of $\underline{\varepsilon}$. In Fig. 2 (a) we plot ε and $\tilde{\varepsilon}$ as functions of h for $\Lambda = 5$. The predicted asymptotic convergence orders are verified. Notice that the error in $\underline{\psi}$ is three orders of magnitude lower than that of $\tilde{\underline{\psi}}$ as soon as K is greater than 32. For coarser meshes, the difference is smaller, but for the full range ε is at least 20 times smaller than $\tilde{\varepsilon}$. Of most interest is the capability of improving the accuracy by increasing the expansion order. Fig. 2 (b) plots ε and $\tilde{\varepsilon}$ as functions of Λ for $h = L/16$. Note that as Λ is increased by one the error decreases by a factor of ten. Also, ε is seen to be smaller than $\tilde{\varepsilon}$ by a factor that ranges from 10 (for $\Lambda = 0$) to 200 (for $\Lambda > 4$).

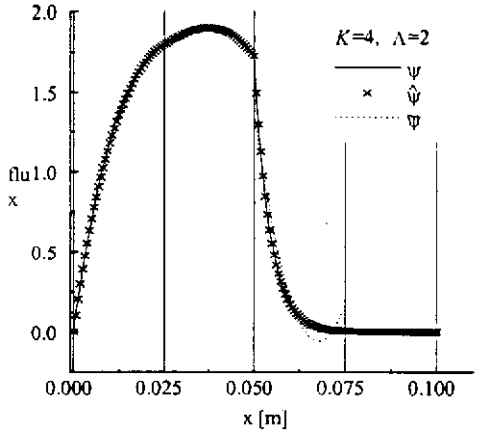

a) Angular fluxes for the K=4 case, Λ =2.

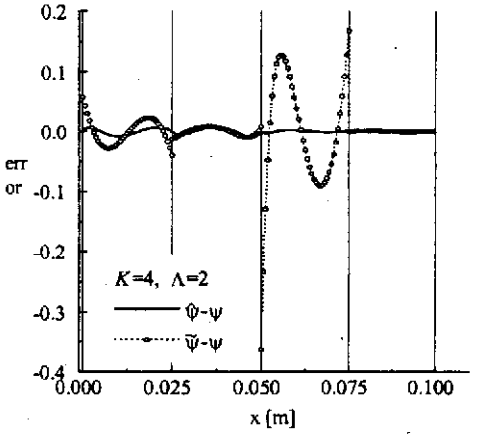

b) Differences between approximate fluxes and exact solution, K=4 case, Λ =2.

Figure 1. Relation between approximate fluxes and the exact solution for the K=4 case, Λ=2.

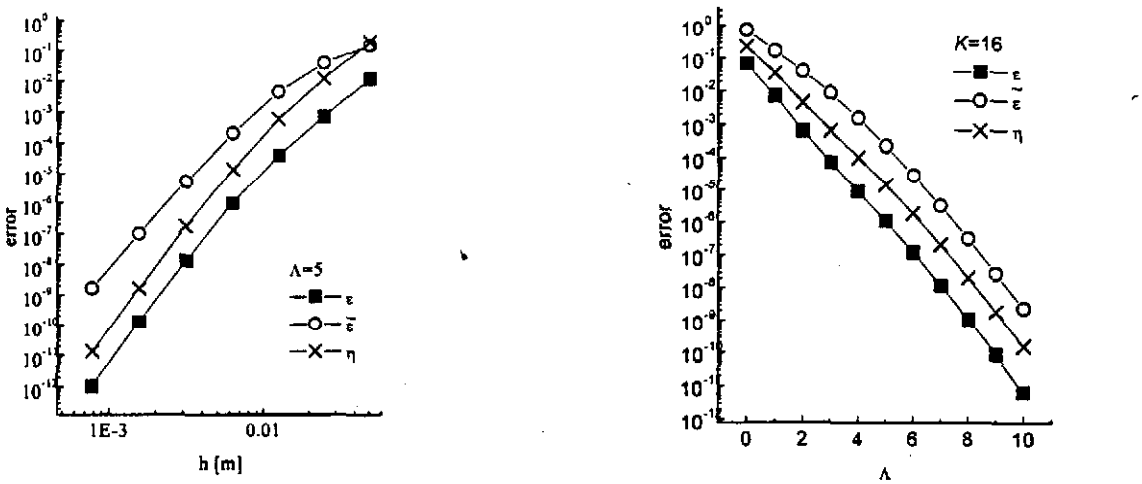

a) ε and $\tilde{\varepsilon}$ as function of h for $\Lambda = 2$. b) ε and $\tilde{\varepsilon}$ as function of Λ

Figure 2. Errors of approximate solutions in L^2 norm.

Numerical tests of *a posteriori* error estimators are aimed at showing that it behaves like the true error. In this case we address three types of behavior: The first one concerns the evolution of η and ε as functions of h for fixed Λ. This is shown in Fig. 2 (a). The estimator correctly follows the error, showing that the higher order terms in Eq. (6) can be disregarded. A second assessment concerns the evolution of η with increasing Λ for fixed h. This is shown in Fig. 2 (b). The resemblance of the curves corresponding to the estimator and the true error is remarkable. The theory considers $h \to 0$, so that this could not be predicted beforehand. To summarize, the results in Fig. 2 give us confidence on that, when the approximation is refined, if the estimator decreases by some factor, the true error has also decreased by approximately the same factor.

For adaptivity purposes a third behavior is important, namely, for fixed h and Λ, the distribution of the estimated error over the cells. This allows improving the approximation only where it is most needed. In Fig. 3 (a) the true error and the local indicators are plotted, computed using 16 cells and an expansion order of 4. The same is done in Fig. 3 (b) for 64 cells and $\Lambda = 6$. Both graphs show that the local indicators follow closely the distribution of the true error over the domain. The most critical cell is the one adjacent to $x=L/2$ from the

right, and adaptive procedures using the proposed indicator would refine this region. By comparing Figs. 3 (a) and (b), notice the high accuracy of the computation with $h=L/16$ and $\Lambda = 4$, which is improved by about six orders of magnitude when $h=L/64$ and $\Lambda = 6$, though the number of unknowns has just increased by a factor of 6.

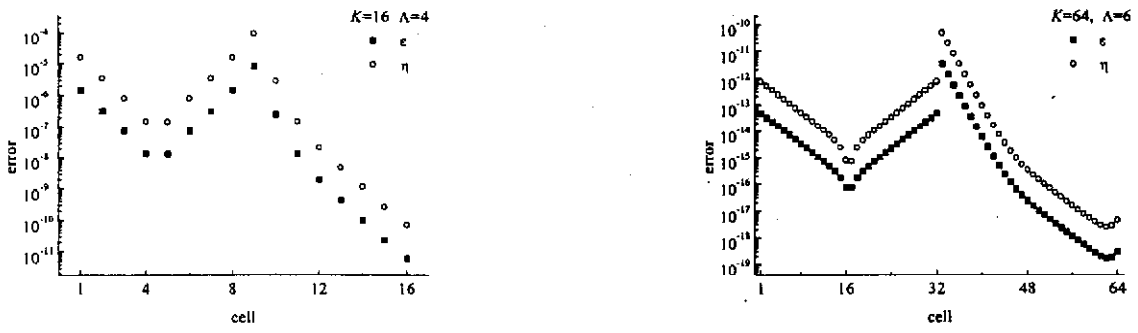

a) True error and indicator for K=16, $\Lambda = 4$.

b) True error and indicator for K=64, $\Lambda = 6$.

Figure 3. Behavior of the true error and indicator as function of the position.

REFERENCES

[1]Azmy, Y., "The Weighted Diamond-Difference Form of Nodal Transport Methods", *Nuclear Sci. Engn.*, **98**, 29-40 (1988).

[2]Larsen, E., Miller, W. "Convergence Rates of Spatial Difference Equations for the Discrete-Ordinates Neutron Transport Equations in Slab Geometry", *Nuclear Sci. Engn.*, **73**, 76-83 (1980).

[3]Larsen, E., Nelson, P., "Finite-Difference Approximations and Superconvergence for the Discrete-Ordinate Equations in Slab Geometry", *SIAM J. Numer. Anal.*, **19**, 334-348 (1982).

[4]Victory, H., Ganguly, K., "On Finite-Difference Methods for Solving Discrete-Ordinates Transport Equations", *SIAM J. Numer. Anal.*, **23**, 78-108 (1986).

[5]Vaidyanathan, R., "A Finite Moments Algorithm for Particle Transport Problems", *Nuclear Sci. Engn.*, **71**, 46-54 (1979).

[6]Zamonsky, O., Buscaglia, G. and Azmy, Y., "*A posteriori* error estimation for the One-Dimensional Arbitrarily High Order Transport-Nodal Method", *Annals Nucl. Energy*, to appear.

[7]Noor, A., Babuska, I., "Quality assessment and Control of Finite Element Solutions", *Finite Elem. Anal. Des.*, 3, 1-26 (1987).

[8]Verfurth, R., *A Review of a posteriori Error Estimation and Adaptive Mesh-Refinement Techniques*. Wiley-Tenber Series in Adv. Numer. Math., Stuttgart (1996).

[9]Jatuff, F. E., "Error Estimators and Adaptivity for the Neutron Diffusion Problem", *Annals Nucl. Energy*, **22**, 775-886 (1995).

[10]Jatuff, F. E., Gho, C. J., "On *a posteriori* Error Estimators: a One-Dimensional Nodal Diffusion Adaptivity Case", *Annals Nucl. Energy*, **24**, 543-552 (1997).